3-1999

Long Simulation of Regional Climate as a Sequence of Short Segments

Zaitao Pan
Iowa State University

Eugene S. Takle
Iowa State University, gstakle@iastate.edu

William J. Gutowski Jr.
Iowa State University, gutowski@iastate.edu

Richard Turner
Iowa State University

Long Simulation of Regional Climate as a Sequence of Short Segments

ZAITAO PAN

Department of Agronomy, Iowa State University, Ames, Iowa

EUGENE TAKLE AND WILLIAM GUTOWSKI

Department of Agronomy and Department of Geological and Atmospheric Sciences, Iowa State University, Ames, Iowa

RICHARD TURNER

Department of Agronomy, Iowa State University, Ames, Iowa

(Manuscript received 3 July 1997, in final form 23 March 1998)

ABSTRACT

Regional climate simulations are long time integrations over an open system where the atmosphere over part of the model domain (boundary zones) is updated periodically. Model reinitialization after a long period of integration can allow several segments of a long simulation to be run in parallel and also minimize possible drift caused by accumulated model errors. However, the spinup problems introduced by each additional restart must be addressed. The necessity and feasibility of subdividing long integrations is investigated by means of a series of experiments in which the authors examine the effects of reinitialization frequency and the relative importance of surface forcing and atmospheric forcing. It is found that for integrations that continued without reinitialization, locations of specific meteorological features drifted downstream because simulated winds were too strong, implying the need for periodic reinitialization of the model. The results indicate also that when the model reinitialization interval is relatively long, simulated domain-averaged variables, including rainfall, were not very sensitive to model reinitialization since they are largely constrained by transient boundary conditions, suggesting the feasibility of dividing long regional climate simulations into a set of shorter ones that could be run in parallel.

1. Introduction

Simulations of climate by regional models, like simulations of global climate, require integrations over several model years. High-resolution and detailed parameterizations can make the computational cost greater for regional climate simulations than for global simulations. An advantage of such long integrations is the continuous representation of the long-term forcing. One such long-term forcing is soil moisture (Beljaars et al. 1996; Betts et al. 1994), which introduces seasonal or even interannual memory. In some sense, the atmospheric forcing by soil moisture over continents is similar to that of sea surface temperature (SST) over oceans. In fact, a partial cause for the 1993 Midwest Great Flood can be traced back to the wet soil in the winter of 1992 and spring of 1993 (Rodenhuis et al. 1994; Mo et al. 1995).

It is possible, however, that the model atmosphere in regional climate models (RCMs) may drift or decouple from its lateral boundary forcing fields provided by general circulation models (GCMs) or observations. The RCMs tend to separate or decouple from GCMs during the integration, especially when the integration domain is large (Kida et al. 1991; Paegle et al. 1996). Model errors, inaccurate numerics, and errors in physical parameterizations create artifacts that may remain in the domain for a long time. Although the model atmosphere is constrained by the boundary conditions provided by either GCMs or observations, differences between the simulated and observed (input) atmospheres can still persist throughout the integration, especially far from the boundaries. These errors can then affect accumulated variables such as rainfall, although they may not noticeably affect the simulated atmospheric states at the end of the simulation.

Possible drift from forcing fields can be avoided if the longwave components in RCMs are nudged frequently to forcing GCMs over the whole interior domain (Kida et al. 1991; Paegle et al. 1996) or the slowly varying variables (e.g., lake and SST) are updated along with the boundary conditions (e.g., Giorgi et al. 1996).

Corresponding author address: Dr. Zaitao Pan, 3010 Agronomy Hall, Dept. of Geological and Atmospheric Sciences, Iowa State University, Ames, IA 50011.
E-mail: panz@iastate.edu

An alternative strategy is to increase the width of the boundary forcing zone where RCM variables are partly provided by the GCM.

RCMs are open systems where the atmosphere over part of the domain (boundary forcing zones) or some components of the model atmosphere must be updated during the course of the integration. In this regard, RCMs are different from GCMs where no part of atmospheric information in the model has to be updated except for external forcing. A question arises as to how much information from the past is still left in the model system after a certain period of integration, especially when the interior domain is not large compared to the forcing zone. If very little previous information is left, we can break a long simulation into shorter ones, and thus both cost and wall-clock time could be reduced by performing regional climate simulations on collections of workstations rather than on supercomputers. These independent segments can be perfectly scalable across all computer platforms since they all have the same problem size.

Soil moisture is a long-term forcing in climate simulations. It may be argued that frequent restarts of the model would interrupt this long memory or alter its spatial distribution through rainfall–soil interaction. The effects of this interruption need to be determined if frequent restarts are to be employed. It is noteworthy that some previous studies have found that the soil-moisture forcing within the model domain tended to be small compared to remote large-scale forcing (Giorgi et al. 1996; Paegle et al. 1996).

This study aims at answering the following questions: 1) Is it appropriate and perhaps necessary to break a long simulation into several short ones, and if so, what are the quantitative effects of the reinitialization on simulations? 2) How important is the surface forcing relative to the atmospheric forcing in RCMs within the context of model reinitialization?

2. Experimental design

The atmospheric fields are considered high-frequency forcing whereas surface variables (primarily soil moisture and deep soil temperature) are considered low-frequency forcing. The modeled atmosphere is periodically updated with observations regardless of their frequencies. This simple updating scheme is an extreme case of spectral nudging approaches (Kida et al. 1991; Paegle et al. 1996). The advantage of this straightforward updating method, in addition to its simplicity, is that it can incorporate observed information on the smallest scales resolved by the forcing dataset, which otherwise might be wasted. This simple updating method also avoids the limitation imposed by Fourier expansion over a *limited domain* associated with the spectral nudging approaches (Renshaw and Ford 1983).

We performed nine experiments as listed in Table 1 where each experiment is labeled as $Y \times N$D with Y being the number of segments in the overall run and N the length of the segments in days. For example, experiment 3×10D is the collection of three successive segments of 10 days in length. Integrations in all experiments except for the 1×20D were carried out for 30 days. The first experiment, 1×30D, was integrated for 30 days without any reinitialization and served as the control. In the second experiment, 3×10D, all the model fields including soil moisture were reinitialized by observations every 10 days to test the effects of restart. The frequency of updating is increased further in experiments that restart the simulations every 5 days (6×5D)—the approximate frequency of synoptic events—and every day (30×1D) to maximize the effects of reinitialization. If the model updates too frequently, spinup problems may be severe; on the other hand, if the integration is too long, the model fields may drift from actual observations. This range of updating frequency allows us to explore the relative effects of spinup and drift.

TABLE 1. Description of the experiments.

Description	Name	Remarks
No reinitialization	1×30D	Climatological M at start
Reinitialize model every 10 days	3×10D	Climatological M at start
Reinitialize model every 5 days	6×5D	Climatological M at start
Reinitialize model every 1 day	30×1D	Climatological M at start
Same as 3×10D but overlap	3×13D	Climatological M at start
Start at 10th day	1×20D	Climatological M at start
Soil is uninterrupted	3×10DS	Climatological M at start
Saturated soil	1×30DW	$M = 1$ over flood area
Dry soil	1×30DD	$M = 0.05$ everywhere

Effects of spinup and related adjustment (Yap 1995) are minimized, in the fifth experiment, 3×13D, where the model is reinitialized every 10 days, but with a 3-day overlap with the previous 10 days. Each segment thus consists of 13 days. The 3-day overlap period at the start of the second and third 13-day segments presumably contains the spinup effects and thus is disregarded for comparison with the control experiment. The effects of starting point on the integration are examined in experiment 1×20D, which was initialized from observations on the 10th day of the 30-day period and run without subsequent reinitialization.

Reinitialization effects may be attributed to updating the atmospheric states or to updating surface forcing. Experiment 3×10DS tests the effects of atmospheric and surface forcing separately by resetting the model atmosphere to the observed state every 10 days, while retaining continuously simulated soil moisture. This allows us to determine the relative impacts of the atmospheric and surface-forcing updating.

The effects of soil moisture are further examined by two experiments specifying the surface as wet ($1 \times$

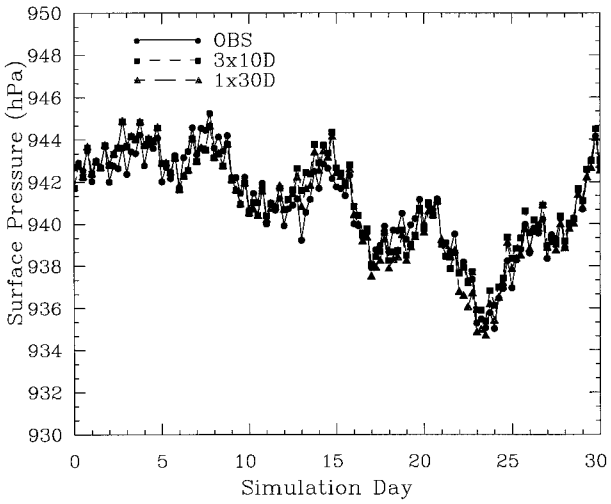

FIG. 1. Time series of domain-averaged surface pressure for 3 × 10D and 1 × 30D experiments as compared with observation.

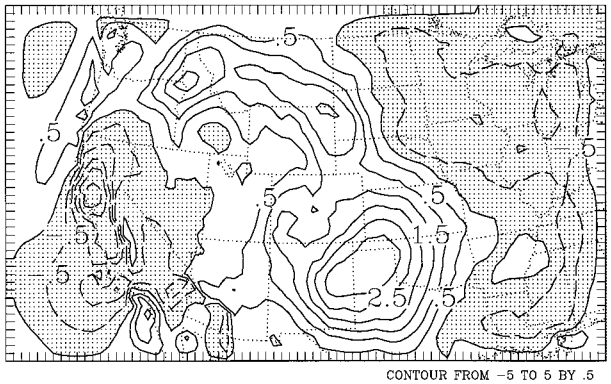

FIG. 2. Spatial distribution of difference (hPa) in surface pressure between the simulation and observation for the 1 × 30D experiment. Areas with negative values are shaded.

30DW) and dry (1 × 30DD). In 1 × 30DW, the soil is set to the saturation level over the 1993 flood area along the Mississippi River basin. This experiment is similar to that used in Giorgi et al. (1996) where soil over the entire domain was prescribed as saturated. In 1 × 30DD soil moisture availability is set to 0.05 everywhere as an extreme contrast of the saturated case.

3. Model and boundary conditions

The regional climate model used in this study (RegCM2) was developed at the National Center for Atmospheric Research (NCAR) based on the Pennsylvania State University/NCAR Mesoscale Model version 4 (Giorgi et al. 1993a, 1993b). The model incorporates the Community Climate Model Version 2 radiation package (Briegleb 1992) and Biosphere–Atmosphere Transfer Scheme (BATS) version 1e (Dickinson et al. 1992) surface package. The model domain is covered by 45 × 76 × (50 km)^2 grids centered at (40.5°N, 106.5°W) with 14 layers in the vertical. The simple Kuo (Kuo 1974; Anthes 1977) scheme is used for most simulations, whereas the relatively sophisticated Grell (Grell 1993) cumulus parameterization scheme is also tested for intercomparison.

Climatological soil moisture availability (M) was used except for 1 × 30DW and 1 × 30DD where soil moisture was set to the saturation and dry values, respectively. The setting of M in 1 × 30DW can be roughly justified because of the long length of the flood period. Additionally this setting is consistent with the observed Palmer Drought Index and Crop Moisture Index (Pan et al. 1995).

The integration covers the period from 0000 UTC 11 June to 0000 UTC 11 July 1993, the peak period of the Midwest Great Flood (Bell and Janowiak 1995). During this eventful period, both physical and dynamic processes (e.g., surface hydrology and precipitation physics) have prominent roles, thereby providing a revealing test of model physics.

The initial and boundary conditions were interpolated from European Centre for Medium-Range Weather Forecasts T42 analyses. These analyzed fields are consistent and in balance with each other reasonably well compared with raw observations. No further adjustment was done to the initial and boundary conditions although the spatial interpolation to our model resolution may introduce slight imbalance. After the model restarts, the predicted variables were nudged to the observations within the buffer zone of width 500 km where the tendencies of predicted variables are updated every 6 h (Giorgi et al. 1993b).

4. Effects of initialization frequency

a. Surface pressure

Regional climate simulations may require a large number of time steps and are therefore vulnerable to accumulation of numerical errors. Conservation of domain total mass, determined from surface pressure, is one measure of the accumulation of errors. The temporal variation of whole domain-averaged pressure shown in Fig. 1 exhibits the passage of several synoptic waves, the strongest of which was on day 23, when the heaviest rainfall occurred over the Midwest. Both the 3 × 10D and 1 × 30D experiments produced surprisingly accurate temporal variation of surface pressure compared with the observations. In fact, for the 1 × 30D integration, the pressure prediction in the final 10 days was even more accurate than the first two 10-day periods. The spatial distribution of surface pressure also was reproduced reasonably well, with maximum time-averaged errors of about +3 hPa centered in northern Texas (Fig. 2). The positive bias may weaken the southerly flow over Texas where the low-level jet frequently occurs. A narrow band of about −2 hPa occurred along the California coast. The overall simulation error in

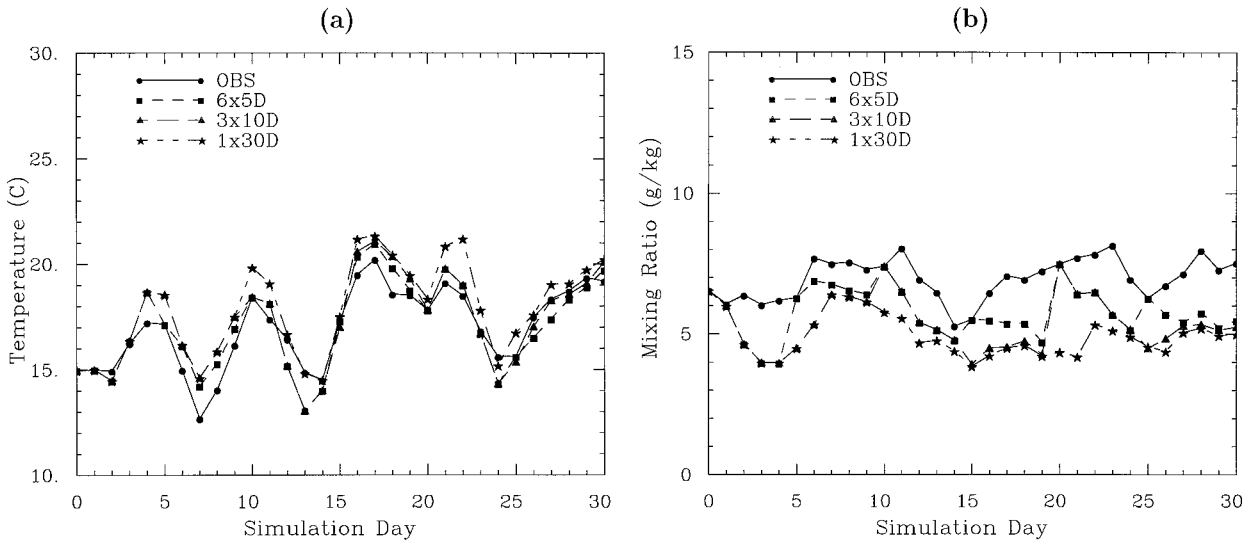

FIG. 3. Temporal variation of simulated interior domain averages as compared with the observation at $\sigma = 0.895$: (a) temperature and (b) mixing ratio.

pressure is about 0.5 hPa. The good agreement between the observed and forecast surface pressure fields is somewhat expected since the pressure systems that dominate synoptic-scale phenomena are manifestations of large-scale waves, which are well resolved by the external forcing data. Other experiments (not shown) simulated similar distributions of surface pressure.

b. Upper-air fields

Figure 3 shows the temperature and mixing ratio at the 11th model level ($\sigma = 0.895$) averaged over the interior domain, which excludes the boundary forcing zones. In RegCM2 the vertical coordinate is

$$\sigma = \frac{p - p_t}{p - p_s}, \tag{1}$$

where p is pressure at a particular model level, p_t is the pressure at model top (=80 hPa), and p_s is the surface pressure. The 11th level is at about 900 m above the ground near the center of the model domain.

The interior domain-averaged temperatures at the 11th level followed very similar trends among different experiments, and they captured the observed temporal variation reasonably well (Fig. 3a). A 1–2-K positive bias was present most of the time with largest simulation errors occurring during cold periods. The restart helped reduce the errors temporarily in the first 2–3 days. All three runs (1×30D, 3×10D, and 6×5D) produced water vapor mixing ratios at the 11th level that were too low (Fig. 3b). Shocks (deviations from the nonrestart run) resulting from the restart were larger and lasted slightly longer in the mixing ratio compared to the temperature and winds at the same level. It took about 4 days for the effects of the restart to fade out. Thus the restarts helped reduce the prediction errors, especially for atmospheric moisture, which had larger model errors.

The small variation of domain averages with different reinitialization frequency does not necessarily imply insensitivity for a particular location or subregion. Domain totals and averages depend mostly on boundary conditions, whereas weather at individual points or over small regions depends on the internal model physics and dynamics. We checked the time series of wind speed, temperature, and mixing ratio simulated by different experiments at a grid near the observed rainfall center. Like the domain average, they all followed trends similar to the observations although with some individual differences (not shown).

The simulated winds at the 11th level were too strong compared with observations with maximum error of about 8 m s^{-1} (Fig. 4a). These excessive wind speeds may be due to model deficiency in boundary layer parameterization. The winds simulated at $\sigma = 0.51$ (about 500 hPa), which is above the boundary layer, are much closer to the observations (Fig. 4b).

The insensitivity of domain-averaged properties to different restart frequencies can be explained by the fact that the average properties over the whole domain are largely constrained by boundary conditions. The initialization does not significantly change the ''fluxes'' at the boundaries, which are mostly determined by observations.

The 30-day time-averaged observed wind fields at $\sigma = 0.895$ were dominated by a strong trough in the western United States and a low-level jet over the central United States where the flood occurred (Fig. 5a). The predicted (1×30D) flow pattern, as indicated by the vector difference between the prediction and observa-

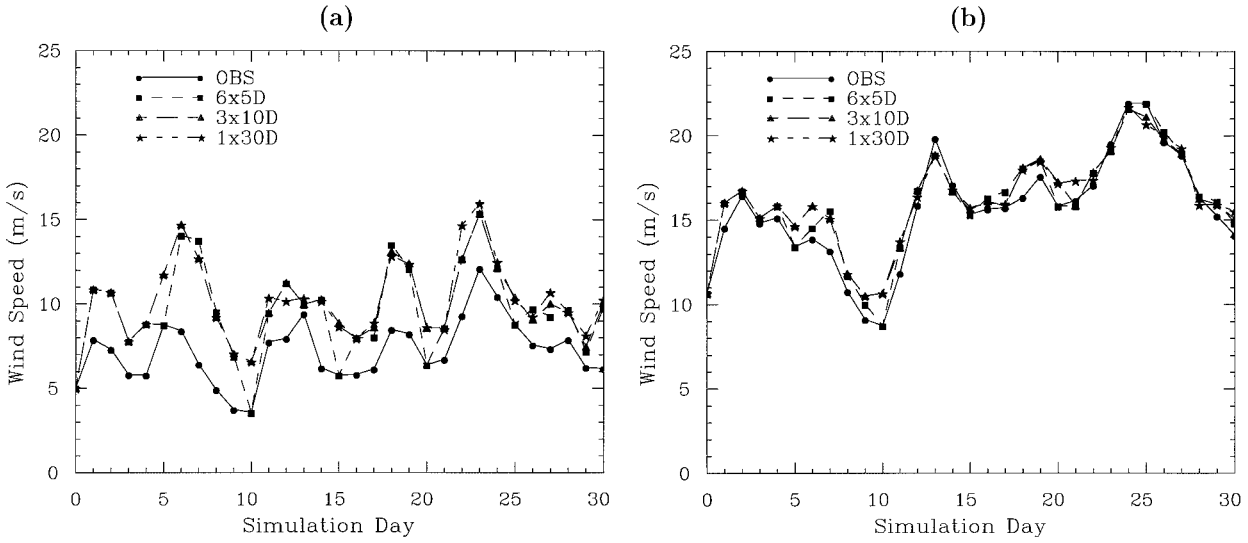

FIG. 4. Temporal variations of simulated and observed wind speeds averaged over the interior domain: (a) $\sigma = 0.895$ and (b) $\sigma = 0.510$.

tion in Fig. 5b, had stronger southerlies over the western United States and westerlies over the Midwest and Great Lakes region. The stronger southwesterlies over the flood area produced a downstream displacement of the rainfall area in the 3 × 10D and 1 × 30D experiments (shown later in this report). It should be mentioned that larger errors in the lee area of the Rockies could result from vertical interpolation near steep mountains.

Correct representation of energy spectra is essential for regional climate simulations. We decomposed the wind fields by a two-dimensional Fourier transform:

$$f(x, y) = \sum_{m=0}^{\infty} \sum_{n=0}^{\infty} D_{m,n} \times \exp\left[i\left(\frac{2\pi m}{S}x + \frac{2\pi n}{T}y\right)\right], \quad (2)$$

where

$$D_{m,n} = \frac{4}{ST} \int_{-S/2}^{S/2} \int_{-T/2}^{T/2} f(x, y) \times \exp\left[-i\left(\frac{2\pi m}{S}x + \frac{2\pi n}{T}y\right)\right], \quad (3)$$

where $f(x, y)$ represents an arbitrary two-dimensional variable, $D_{m,n}$ is the corresponding Fourier coefficient, S and T are the domain lengths in the east–west and north–south directions, and m and n are the wavenumbers in the east–west and north–south directions, respectively. As an example, Fig. 6 shows the time-averaged wave amplitude ($D_{m,n}^2$) of u-component winds at the seventh level ($\sigma = 0.510$). The T42 representation of the observations sharply concentrated energy at the longer wavelengths (smaller wave number) in both east–west and north–south directions (Fig. 6a). The 3 × 10D simulation gave a much wider spectrum than the T42 analysis, indicating the presence of more small-scale motions (Fig. 6b). Thus, the model indeed generated mesoscale features when forced by the large-scale fields at the boundaries. A wind spectrum similar to the 1 × 30D run was obtained for the 3 × 10D simulation.

Renshaw and Ford (1983) suggested that decomposition by one-dimensional Fourier transformation provides a clearer view of spectral behavior. The simulated one-dimensional spectrum had more power in shorter waves (Fig. 7), with the 1 × 30D results having slightly more power than those for 3 × 10D for short wavelengths in the east–west direction. The simulated winds had noticeably more power than the T42 analysis.

c. Spatial distribution of rainfall

Rainfall is the end product of numerous atmospheric processes and can be very sensitive to model configuration and atmospheric state. The spatial distribution of observed 30-day accumulated rainfall in Fig. 8a reveals a heavy-rainfall area with over 200 mm centered on southern Iowa and covering most neighboring states. An elongated center of heavy rainfall was observed near the Nebraska–Missouri border and produced more than 300 mm of rainfall averaged over the grid box (with a maximum of 530 mm at one station). Daily reinitialization (30 × 1D) reproduced the heavy rainfall area with similar shape and location, although the amount and extent were larger. The rainfall center observed in northeastern Kansas was shifted northward to central Iowa in the simulation (Fig. 8b). The main rainfall center in the 6 × 5D (Fig. 8c) and 3 × 10D (Fig. 8d) experiments shifted downstream (northeastward) to eastern Iowa and western Wisconsin, respectively. In the 1 × 30D simulation (Fig. 8e), there was no well-defined rainfall center in the flood area and rainfall was more scattered. The center of maximum rainfall shifted eastward to the Great Lakes region, and only about 200 mm

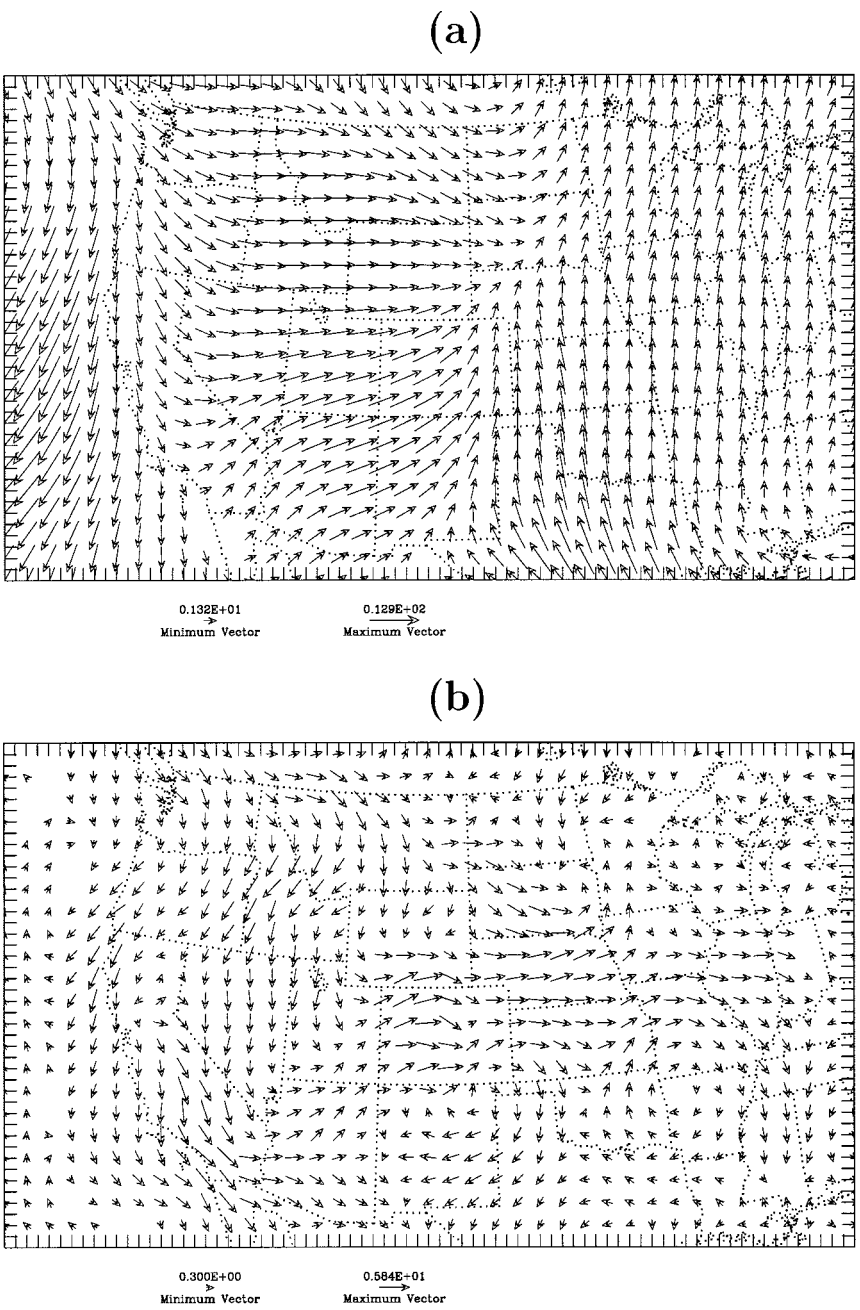

FIG. 5. Spatial distribution of observed (a) and difference between simulated (1 × 30D) and observed (b) wind vectors (m s^{-1}) at $\sigma = 0.895$ averaged over the 30-day period.

of rainfall was simulated compared with an observed rainfall peak of more than 400 mm.

In the 3 × 13D experiment (Fig. 8f), where the first 3 days of simulation for the second and third 13-day periods was disregarded, the rainfall distribution was very similar to that of the control run, 1 × 30D (Fig. 8e). The rainfall distribution, which is one of the most sensitive variables, is essentially the same for the 30-day continuous run and three separate 10-day runs. This strongly supports the feasibility or even the necessity of breaking long climate integrations into collections of short runs.

Climatologically the rainfall over Montana was probably dominated by large-scale stratiform precipitation instead of the intense convective rainfall observed over the flood areas. All simulations reproduced reasonably well the observed rainfall areas over Montana although the amounts were slightly larger than the observed. This implies that stratiform precipitation driven by large-scale circulation was less sensitive to the initialization

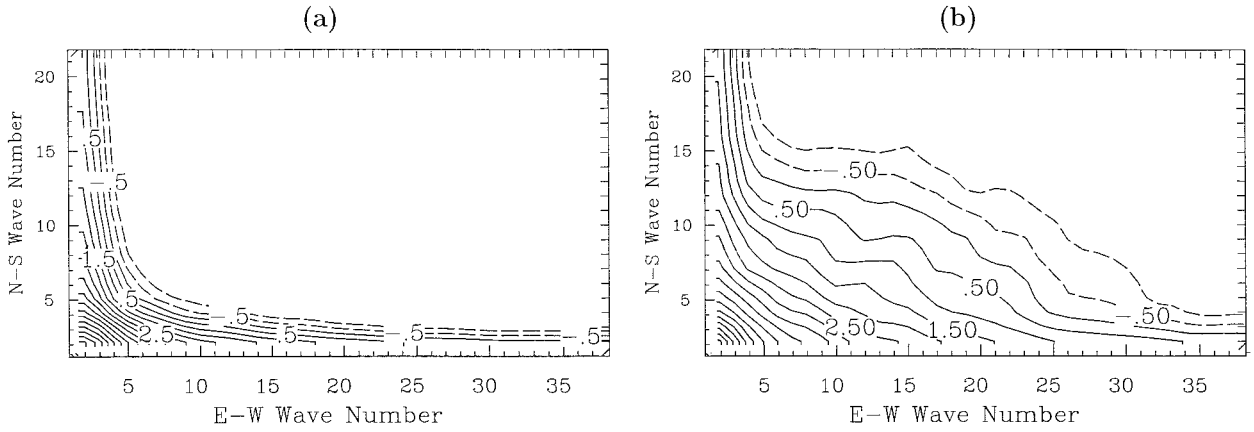

FIG. 6. The 30-day average wave amplitudes (ln $D^2_{m,n}$) of u-component wind at $\sigma = 0.51$ as function of wavenumbers (m, n) in east–west and north–south directions: (a) T42 and (b) simulated (1×30D).

frequency than mesoscale convection. On the other hand, none of these experiments captured the observed rainfall along the Texas–Louisiana coast (possibly due to being too close to the boundaries).

Table 2 lists the peak and 90th percentile rainfall values, location error of rainfall center (the location with maximum rainfall), and threat score (TS) of rainfall over 200 mm. The TS is defined as

$$\text{TS} = \frac{A_C}{A_F + A_O - A_C}, \tag{4}$$

where A_C and A_O are, respectively, areas of correctly forecast and observed rainfall over 200 mm, and A_F is the total forecast area for rainfall over 200 mm. A perfect forecast would give TS $= A_C/A_F = 1$. This table shows that, as reinitialization frequency increases, the location and distribution are better simulated because the wind speeds, which determine the system location and are excessive in the model, were reset to the observations. Downstream drift (position error) of the rainfall area was probably due to excessive wind speeds in the model (as seen in Figs. 4a, 5b, 7). However, the rainfall maximum increases excessively as reinitialization frequency increases due to spinup/overshooting or adjustment of imbalanced variables (Yap 1995).

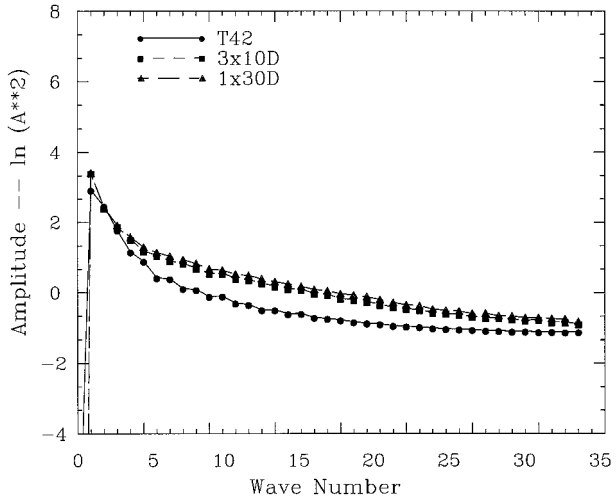

FIG. 7. The 30-day average wave amplitudes (ln A^2) of one-dimensional Fourier decomposition of u-component wind speed at $\sigma = 0.51$.

d. Temporal variation of rainfall

The observed rainfall over the continental United States increased roughly at 2.5 mm day^{-1} over the simulation period (Fig. 9a). The first four experiments in Table 1 simulated essentially the same magnitude of rainfall, all being about 15%–20% smaller than the observed amounts after 30 days. During the first half of the 30-day period, the simulated U.S. continentally averaged rainfall rate was about 2 mm day^{-1}, four-fifths of the observed value, but for the second half of the 30-day period, the simulated rainfall was similar to the measurements. The similar amounts of domain-total rainfall simulated by all experiments indicate that different updating frequencies alter spatial distribution but have little effect on the domain total. This implies that total precipitation, like other variables, is mainly governed by inflow through the boundaries.

The partitioning of total rainfall into convective and nonconvective forms helps us understand model dynamics. The partitioning of rainfall was quite different among different experiments (Fig. 9b) although final accumulations were almost identical. For the 30×1D simulation, about 65% of rainfall was in convective form, whereas the values were about 44%, 40%, and 32% for the 6×5D, 3×10D, and 1×30D experiments, respectively. Thus as integration period increased, rainfall processes shifted from convective to the nonconvective form. The observed rainfall appeared to be mostly convective during this time period. If true, then the 3×10D and 1×30D simulations had a nonconvective bias. Also, the ratios in different experiments

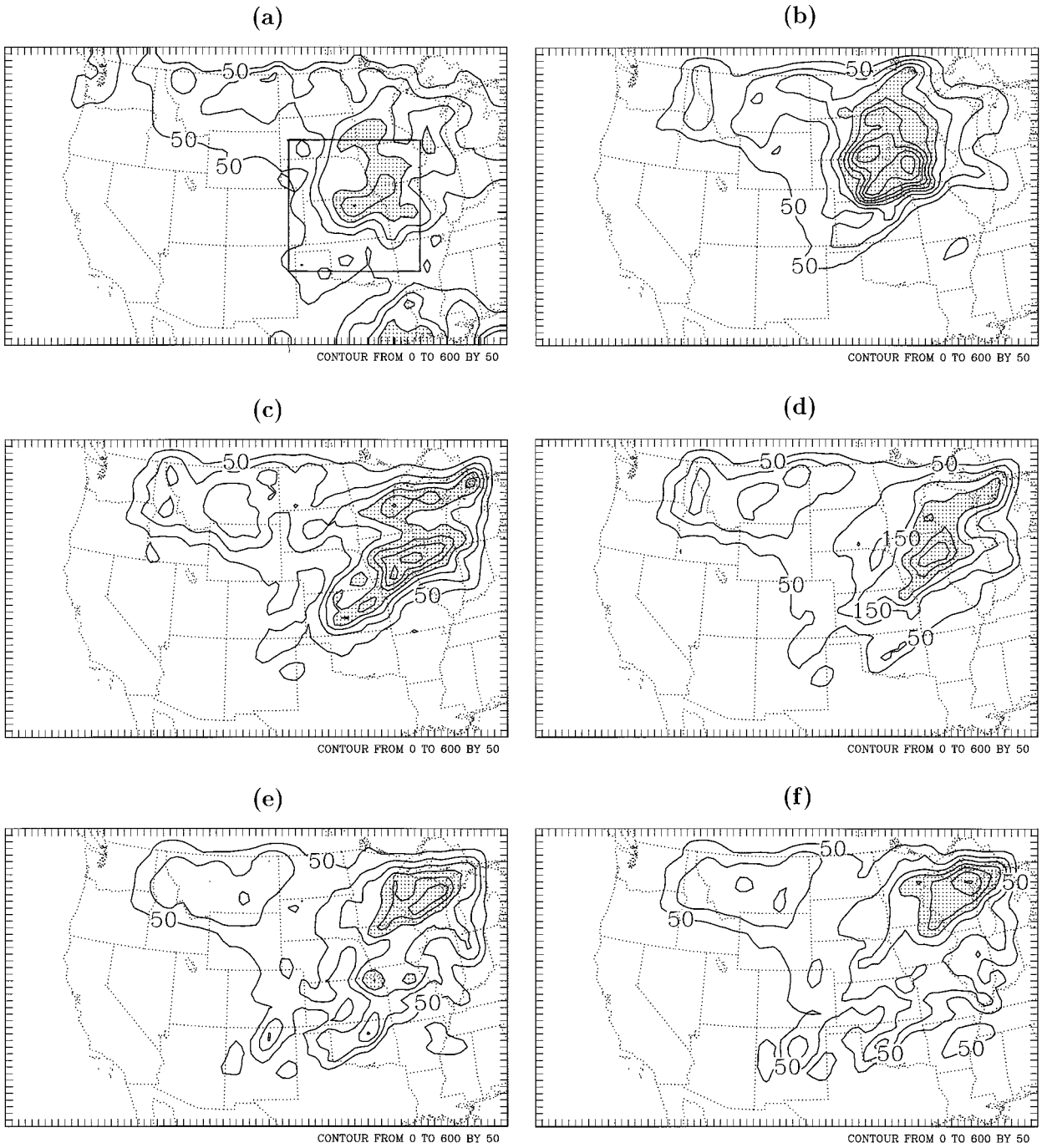

FIG. 8. Spatial distribution of observed and simulated 30-day cumulative rainfall (mm): (a) observed, (the inner square defines the flood area), (b) 30 × 1D, (c) 6 × 5D, (d) 3 × 10D, (e) 1 × 30D, and (f) 3 × 13D. Areas with more than 200 mm are shaded.

were rather steady, implying persistence of the difference. It should be noted that the ratio may not be meaningful for the first few days when rainfall was small.

Domain-averaged rainfall may mask features from individual synoptic systems, so rainfall accumulation over the flood region was analyzed to investigate heavy rainfall events. The flood region defined here covers 1000 km × 1000 km centered at the observed rainfall center in northeastern Kansas (see Fig. 8a).

Flood region average rainfall amounts (Fig. 9c) predicted by the first four experiments were similar to each other and to the observations, but were smaller than the measured values for the entire period except for the 30 × 1D, which gave significantly larger rainfall than all

TABLE 2. Rainfall simulation errors in different experiments.

Variable	1 × 30D	3 × 10D	6 × 5D	30 × 1D	3 × 13D	OBS
Peak rainfall (mm)	328	344	381	475	353	331
90th percentile (mm)	250	236	291	408	255	230
Position error (km)	900	600	500	350	900	0
TS (%)	11	12	26	29	11	100

other simulations as well as the observation. The 30 × 1D run had excessive rainfall during the second half of the simulation period. On the other hand, rainfall differences among the 6 × 5D, 3 × 10D, and 1 × 30D were smaller and did not increase with time. This may be partly explained by the fact that a period of five or more days is beyond the model spinup/overshooting time. The difference between updated and nonupdated model runs occurs mainly within the first couple of days (as seen in Figs. 3, 4), beyond which the atmospheric state is basically determined by the boundary conditions. The 6 × 5D and 3 × 10D simulations gave similar results, implying the spinup problem was shorter than 5 days. The 30 × 1D experiment produced excessive rainfall due to unrealistically intense rainfall simulated during the last 5 days. On the other hand, the other experiments had rainfall similar to the actual values during this 5-day period.

We analyzed 6-h rainfall totals over the flood region to examine the underlying causes. Observed rainfall shows a well-defined diurnal cycle superimposed on the synoptic events (Fig. 10) with intense rainfall occurring during afternoon and evening (1800–0600 UTC) (Table 3). The 30 × 1D simulation produced a stronger daily cycle, but it shifted the diurnal peak toward late morning (1200–1800 UTC). This shift was due to the model spinup effect that minimized rainfall during 0000–0600

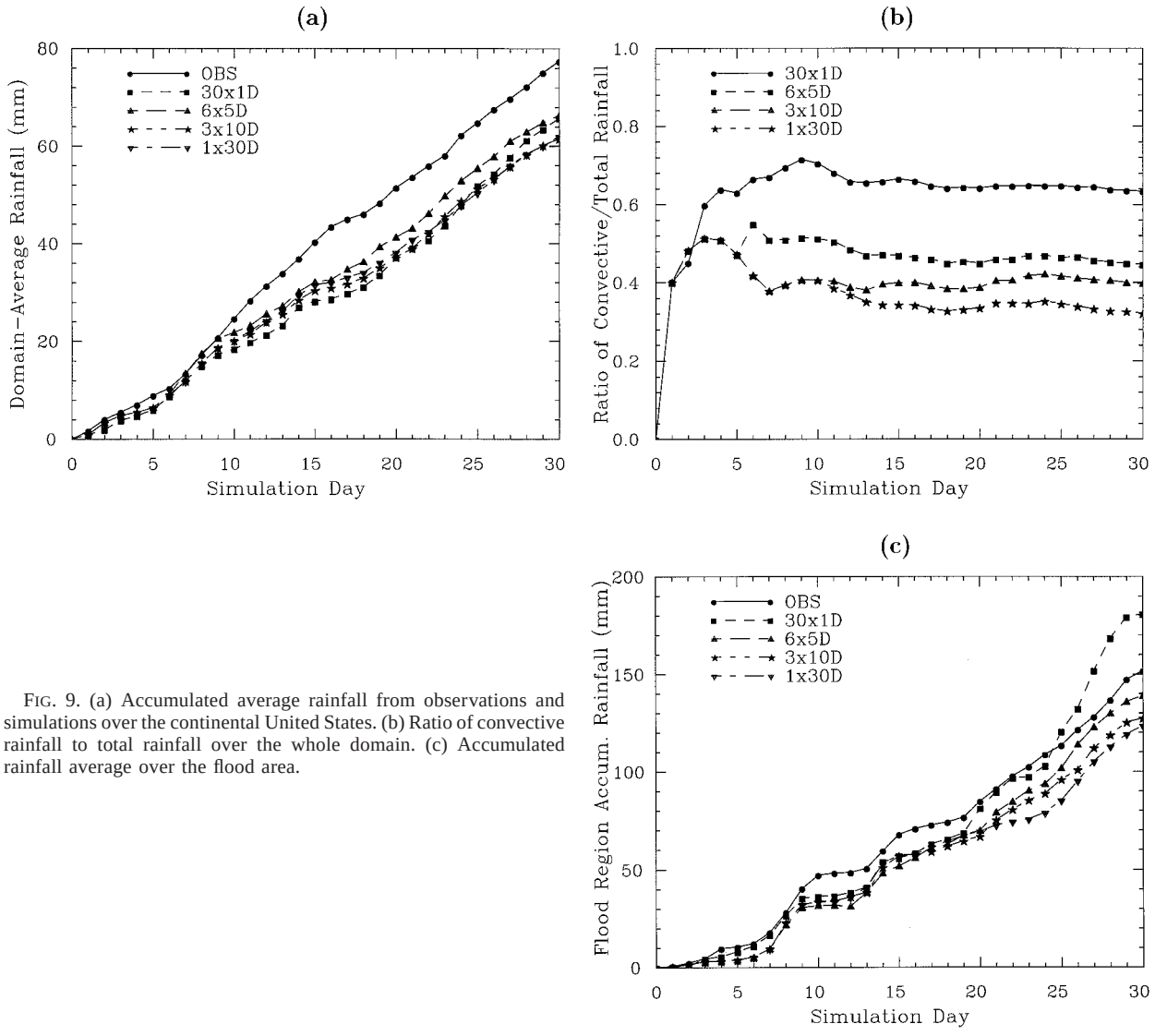

FIG. 9. (a) Accumulated average rainfall from observations and simulations over the continental United States. (b) Ratio of convective rainfall to total rainfall over the whole domain. (c) Accumulated rainfall average over the flood area.

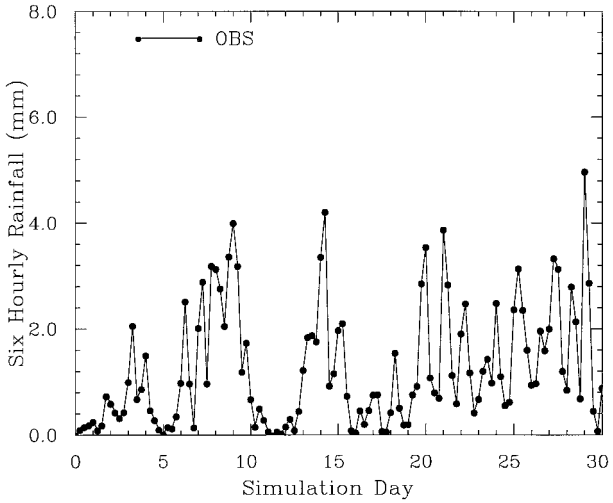

FIG. 10. Time series of domain-averaged observed 6-h rainfall.

UTC. (Integrations in the 30 × 1D run start at 0000 UTC.) The 3 × 10D and 1 × 30D runs simulated only marginal diurnal cycles with peaks tending to occur in early morning (0600–1200 UTC).

Experiment 30 × 1D produced much more rainfall than the others, presumably because its integration period is well within the spinup time. The generally accepted view is that the vertical circulation and precipitation should be weak during the spinup period, but rainfall in this experiment was excessive. Possible explanations are either that the model spinup time in this case was much shorter than 1 day and the related overshooting (Horel et al. 1994) was dominant or that the longer integrations distorted the precipitation processes.

From our previous experience (Pan et al. 1995), the parent model of RegCM2, MM4, develops rainfall rather quickly, within 3–9 h. Once precipitation starts, it intensifies rapidly and then tapers off as the integration proceeds. The model initially tends to adjust all the inconsistencies, such as unphysical convergence, among different variables to achieve a balanced state and may produce spurious rainfall in the process (Horel et al. 1994; Yap 1995). These experiments suggest that the imbalance adjustment affects rainfall more than spinup. This adjustment or overshooting was most evident in the last 5 days of the simulation period when the simulated atmospheric conditions were most conducive to convection. It is responsible for the excessive rainfall seen in Fig. 9c.

The time series of daily rainfall for 3 × 10D, 1 × 30D, and 3 × 13D shown in Fig. 11 reveal differences between the 3 × 10D and 1 × 30D experiments, especially during the first 3 days of restart. This result corroborates the results of the spatial distribution of the simulated rainfall (Figs. 8e and 8f), supporting the validity of dividing a 30-day run into short segments.

Frequent reinitialization keeps rainfall in the correct location (Fig. 8) but produces excessive amounts (Fig. 9) due to the initial adjustment of imbalanced fields. This adjustment mostly affects the rainfall magnitude but not rainfall location. On the other hand, less frequent reinitialization eliminates the spinup/adjustment problem, but allows rainfall locations to shift downwind because of enhanced simulated winds. An intermediate frequency of initialization seems desirable, with the time-overlapping method applied in 3 × 13D being an effective means of eliminating excessive rainfall and downstream shift.

TABLE 3. Six-hourly accumulated rainfall (mm) averaged over the 30-day period (times in UTC).

Expt	0000–0600	0600–1200	1200–1800	1800–0000	UTC
Obs	1.63	0.94	0.91	1.57	
30 × 1D	0.24	1.48	2.12	2.19	
3 × 10D	1.18	1.11	0.96	1.00	
1 × 30D	1.19	1.13	0.89	0.92	

In experiment 1 × 20D, the integration started at day 10. Its 20-day accumulated rainfall (Fig. 12a) was generally similar to that of the last 20 days in 1 × 30D (Fig. 12b). Note that Fig. 12a contains the overshooting in the first couple of days. (Figs. 12a and 12b would have been closer to each other if the overlapping technique had been used in experiment 1 × 20D.) This suggests that rainfall near the end of the simulation period was not sensitive to the starting point of the integration (as long as the spinup/adjustment is avoided). This similarity is reasonable since effects of the initial condition faded after 2–3 days when there were no major rainfall events during the first 10-day period.

5. Effects of reinitializing soil moisture

Long-term forcing due to soil moisture was examined by reinitializing atmospheric variables but keeping soil

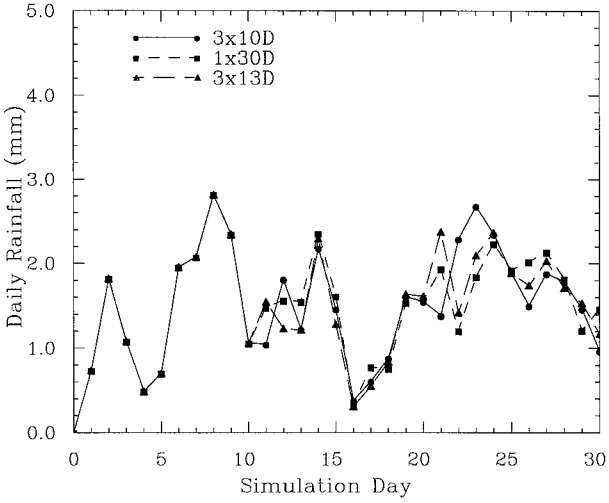

FIG. 11. Time series of domain-averaged simulated daily rainfall.

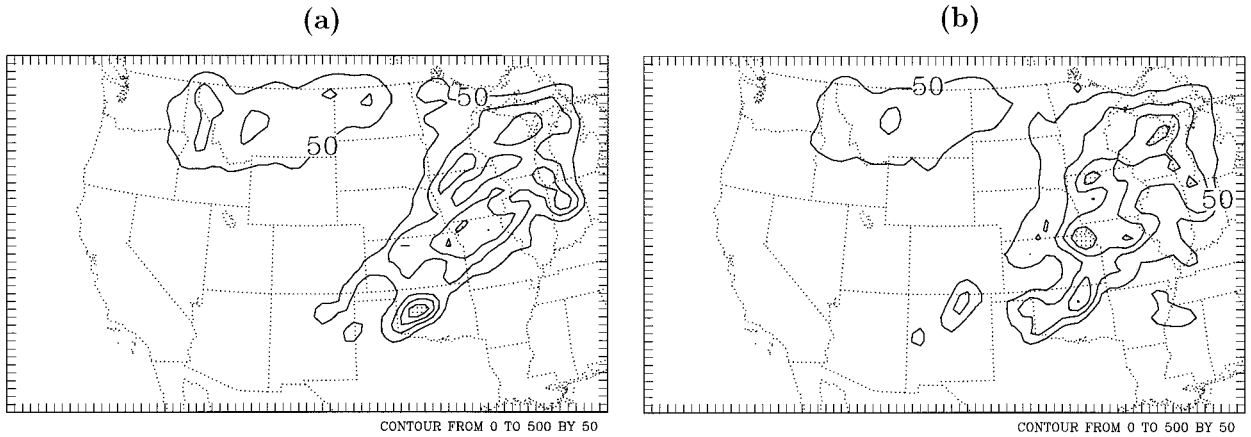

FIG. 12. Spatial distribution of accumulated rainfall (mm): (a) 1 × 20D and (b) last 20 days of 1 × 30D. Areas with more than 200 mm are shaded.

moisture uninterrupted. Figure 13 shows the results from 3 × 10DS where the atmosphere was updated but soil moisture was not interrupted (same as that in the 1 × 30D run). The 3 × 10DS accumulated rainfall is closer to that for 3 × 10D than for 1 × 30D and the maximum rainfall center coincided with that in 3 × 10D (Fig. 8d). The similarity of 3 × 10DS to 3 × 10D results indicates that updating atmospheric forcing had larger impacts than updating surface forcing. The difference in total soil water was less than 2 mm between the experiments with and without soil moisture reinitialization, so soil moisture did not change much between the updated and nonupdated cases. Also, it seems that in BATS as implemented in RegCM2, soil moisture tends to be close to saturation most of the time during this period (F. Giorgi 1996, personal communication).

Figure 14 shows the 30-day accumulated rainfall for 1 × 30DW and the difference between 1 × 30DW and 1 × 30DD (1 × 30DW minus 1 × 30DD). The two experiments produced similar overall patterns of rainfall that also closely resemble the results for the 1 × 30D experiment (Fig. 8e) although substantial differences existed in detail. The difference in domain-average rainfall was 1.8 mm over the 30-day period. The small difference in general pattern between these two experiments suggests the secondary importance of soil moisture memory and provides additional evidence that dividing a long simulation into a collection of shorter runs may not be substantially degraded by loss of soil moisture persistence. Wetting (1 × 30DW) the soil produced more rainfall over the dry western United States and less rainfall over the already wet central United States (Fig. 14b). This is especially true in Oklahoma where the surface is climatologically wet because of land use variety (Fig. 15). The negative correlation between rainfall and soil moisture possibly was due to a strengthened low-level jet over the dry surface (Paegle et al. 1996; Pan et al. 1996).

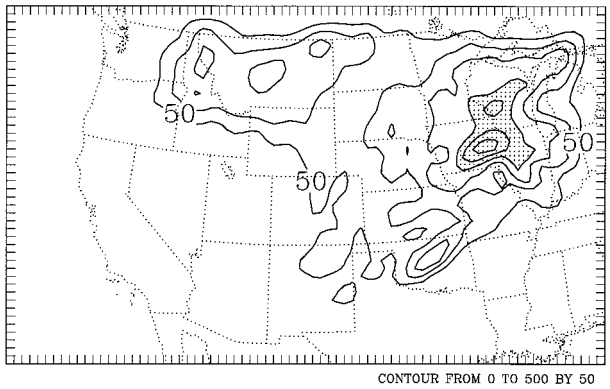

FIG. 13. Spatial distribution of 30-day accumulated rainfall (mm) for 3 × 10DS. Areas with more than 200 mm are shaded.

6. Sensitivity to domain size, parameterization scheme, and climate regime

Some studies have shown that regional climate simulations are sensitive to simulation domain and model convection scheme (e.g., Jones et al. 1995; Giorgi et al. 1993b). We reran experiments 1–4 (1 × 30D, 3 × 10D, 6 × 5D, and 30 × 1D) over a much larger domain using a different cumulus convection scheme and for another climate regime. The domain in this case was 5200 km × 3850 km, 2.5 times larger than the previous domain, and encompasses parts of Mexico, Canada, and neighboring oceans. The Grell cumulus scheme, which has been more widely used in recent years (Grell 1993), was adopted as a contrast to the Kuo scheme. The 1988 drought case was added as a contrast with the 1993 flood case to further examine the sensitivity of simulation results to different large-scale forcing.

Rainfall simulated with the Grell scheme over the much larger domain exhibits features similar to those simulated by the Kuo scheme over the smaller domain. One such feature is that the heavy rainfall area was of

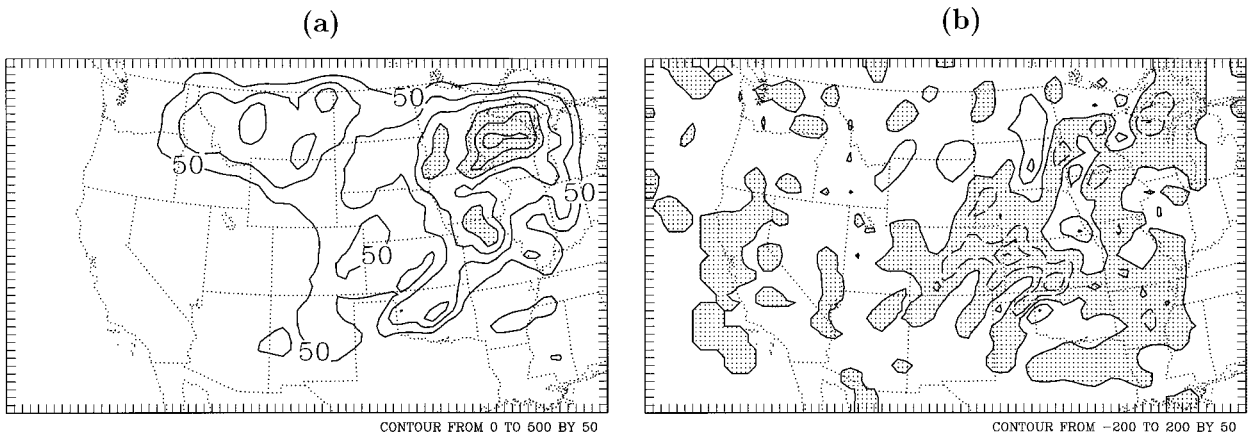

FIG. 14. (a) Spatial distribution of simulated 30-day total rainfall (mm) for 1 × 30DW. Areas with more than 200 mm are shaded. (b) Difference in 30-day rainfall between 1 × 30DW and 1 × 30DD. Areas with negative values are shaded.

similar magnitude and areal coverage and was shifted downstream toward the northeast (Fig. 16), confirming the results obtained from the Kuo scheme using the smaller simulation domain. This tendency of downstream shift was also shown in Giorgi et al. (1996). A second feature revealed in average rainfall accumulation over the continental United States (Fig. 17) is that the rainfall amount decreased as the integration period lengthened. The 30 × 1D simulation produced excessive rainfall, especially during the last 5 days, as seen in previous simulations, although average rainfall simulated is greater than before. A third similarity is that the threat score dependence on initialization frequency is similar but the Grell scheme had a better overall performance (Table 4). The position error was also reduced especially for the 1 × 30D run. The average rainfall was about 25%–30% greater than previous runs, closer to the observation, possibly attributable to the Grell scheme. The slightly wider separation in final rainfall amounts among different experiments (Fig. 17) could be partly explained by the fact that the larger domain allows longer existence of reinitialization effects in the model. In summary, the overall behavior of simulations using the Grell scheme and a larger simulation domain confirms results obtained in previous sections.

The period 0000 UTC 11 June to 0000 UTC 11 July of 1988 (same as the 1993 simulations), which corresponded roughly to the peak of the drought period, was simulated to produce a contrast to 1993 results. As expected, U.S. continentally averaged rainfall is much smaller than 1993 (Fig. 18). The general effects of reinitialization are similar to those for 1993, with largest rainfall being produced by 30 × 1D and smallest by 1 × 30D. One distinct feature in this case is that rainfall accumulation between 3 × 10D and 1 × 30D simulations tended to be parallel, suggesting the difference between the two runs was mainly generated in days 10–15 as a result of the first restart of the simulation. This case again shows the possibility of subdividing the 30-day simulation into three 10-day runs. It is worth noting

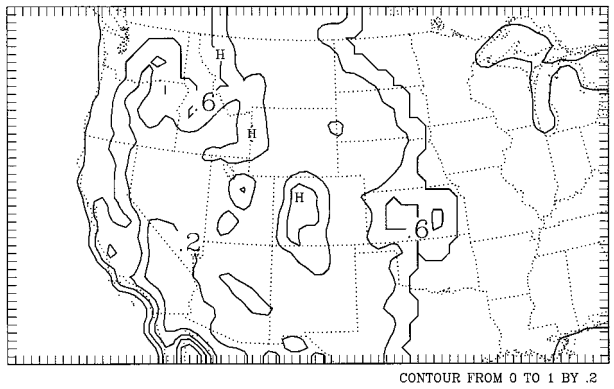

FIG. 15. Climatological soil moisture availability (*M* in fraction of 1) used in the simulations.

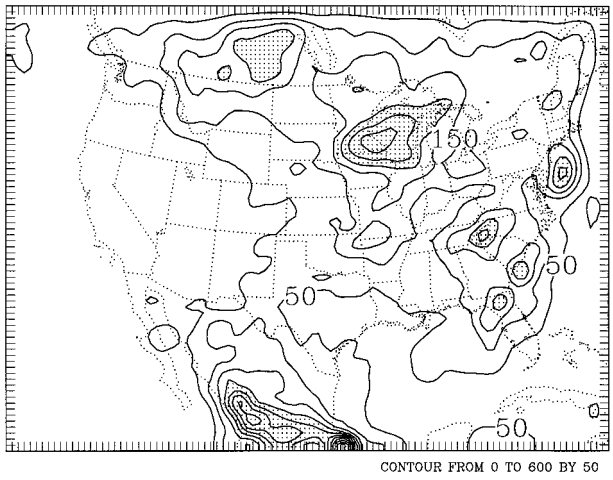

FIG. 16. Spatial distribution of simulated total rainfall (mm) by 1 × 30D using the Grell scheme over a larger domain for 1993 simulations. Areas with more than 200 mm are shaded.

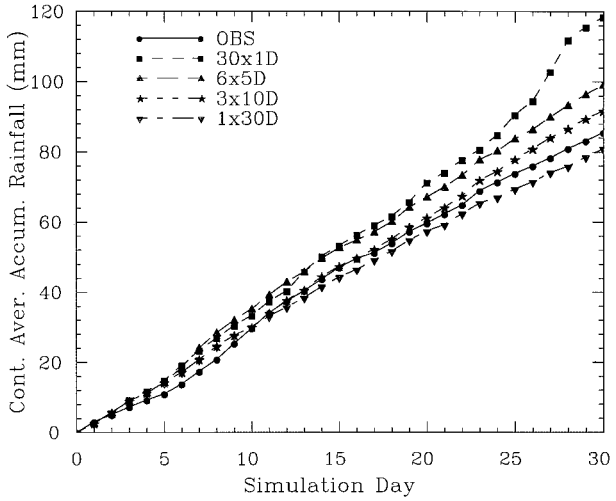

FIG. 17. Accumulated average rainfall over the continental United States for 1993 simulations.

that in all experiments the model has a systematic positive bias in simulated rainfall amount, which is related to model internal features and is independent of restarting procedure. To a large extent, this bias was contributed by so-called single-grid storms that tended to occur when the surface in the Texas and New Mexico area experienced intense heating.

It should be mentioned that unlike the rainfall distribution for the 1993 flood case, rainfall in 1988 did not have a distinct rainfall area, and thus no position error or threat score was given for the 1988 case.

7. Summary and discussion

Long-period simulations of regional climate have the advantage of keeping the long-term forcing uninterrupted. However, the model atmosphere in the domain interior may drift from the forcing observations during the course of long integrations. An optimal reinitialization frequency for the entire domain will retain sufficient long-term forcing and improve the accuracy of the simulated fields. Long-term complete domain reinitialization offers the possibility of dividing long-term simulations into a collection of independent simulations that could be run on a cluster of workstations to speed the simulation and reduce cost.

A series of experiments reported in this study allowed us to evaluate the impacts of complete domain reinitialization at various frequencies. The results showed that in continuous integrations without updating the domain interior, meteorological features drifted downstream because the simulated winds were too strong. On the other hand, when reinitialization was too frequent, excessive rainfall was produced owing to spinup/adjustment, although the positioning of rainfall area was improved.

The results showed that *domain-averaged* winds, temperature, mixing ratio, and rainfall were not sensitive to reinitialization as long as the model was not restarted so often. The total mass, rainfall, and average winds over the domain were similar during the 1-month period whether the model integration was interrupted every 5 days, 10 days, or not at all. This suggests that domain-averaged properties are mainly constrained by boundary conditions.

TABLE 4. Rainfall simulation errors in different experiments using the Grell scheme over the large domain.

Variable	1 × 30D	3 × 10D	6 × 5D	30 × 1D	Obs
Peak rainfall (mm)	351	352	409	709	331
Position error (km)	700	550	650	550	0
TS (%)	14	17	34	31	100

The spatial and temporal distributions of various variables were somewhat sensitive to the frequency of model reinitialization for individual synoptic events. These effects were found to be attributable to atmosphere updating rather than to soil moisture updating, even though the model atmosphere advects out of the model domain within a few days whereas soil moisture influences the model throughout the integration. The secondary importance of surface forcing (long memory variable) provides an opportunity to subdivide a long simulation into shorter ones.

Soil moisture is one of the most poorly observed variables and is usually very crudely represented in most models. Climatological or arbitrarily specified values are commonly used for soil moisture content. Errors introduced by the interruption of long-term forcing from soil moisture are probably well within the range of uncertainty associated with soil moisture specification.

Differences or shocks in simulated fields among the experiments with different initialization frequencies are mainly limited to 2–3 days after restart. These shocks,

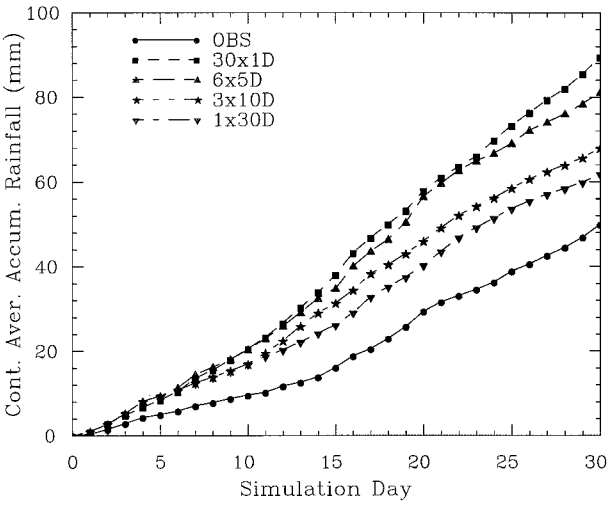

FIG. 18. Accumulated average rainfall over the continental United States for 1988 simulations.

which are caused by the imbalance adjustment, can be eliminated by using a short overlap period. Shocks due to reinitialization can be enhanced by intense rainfall events through a secondary interaction of soil moisture with the atmosphere. Therefore, a simulation should not be reinitialized during periods of intense precipitation. This means that the individual segments may need to be of unequal length.

In summary, it should be and seems feasible to divide a long regional climate simulation into a collection of shorter ones, provided 1) the minimum simulation interval is long enough to minimize the spinup/adjustment problem, and 2) the break point does not occur during a period of intense rainfall. The overlapping procedure may also be useful for reducing spinup effects. This study has shown that even a relatively short 1-month period can be subdivided without sacrificing accuracy for the domain average. From a purely computational efficiency point of view, dividing a multimonth simulation into multiple 1-month runs with a few days of overlap will introduce differences that are negligible compared to uncertainties associated with other components of the model. Such a procedure would also allow use of a cluster of smaller computers in lieu of a supercomputer, thus reducing considerably the cost and time associated with completion of the simulations.

Acknowledgments. This is Journal Paper J-17633 of the Iowa Agriculture and Home Economics Experiment Station, Ames, Iowa (Project No. 3153). The authors thank Ms. Christine Shields, who kindly provided part of the initial and boundary conditions and patient consultation on the RegCM2 code. We are thankful to Dr. Filippo Giorgi for his valuable advice. Helpful discussions with Chris Wikle and Moti Segal are also highly appreciated. Careful review and insightful suggestions from Dr. Raymond Arritt and three anonymous reviewers are highly appreciated. Part of the computer support used in this study was provided by the Climate Simulation Laboratory of the National Center for Atmospheric Research sponsored by the NSF. Financial support for this study was provided by NSF Grant ATM-9627890, the Electric Power Research Institute Contract 4446-03, and NASA Grant NAG 5-2491.

REFERENCES

Anthes, R. A., 1977: A cumulus parameterization scheme utilizing a one-dimensional cloud model. *Mon. Wea. Rev.,* **105,** 270–286.

Beljaars, M. C., P. Viterbo, and M. J. Miller, 1996: The anomalous rainfall over the United States during July 1993: Sensitivity of land surface parameterization and soil moisture anomalies. *Mon. Wea. Rev.,* **124,** 362–383.

Bell, G. D., and J. E. Janowiak, 1995: Atmospheric circulation associated with the Midwest floods of 1993. *Bull. Amer. Meteor. Soc.,* **76,** 681–695.

Betts, A. K., J. H. Ball, A. C. M. Beljaars, M. J. Miller, and P. Viterbo, 1994: Coupling between land and surface boundary layer parameterizations and rainfall on local and regional scales: Lessons from the wet summer of 1993. Preprints, *Fifth Symp. on Global Change,* Nashville, TN, Amer. Meteor. Soc., 174–181.

Briegleb, B. P., 1992: Delta-Eddington approximation for solar radiation in the NCAR Community Climate Model. *J. Geophys. Res.,* **97,** 7603–7612.

Dickinson, R. E., A. Henderson-Sellers, and P. J. Kennedy, 1992: Biosphere-Atmosphere Transfer Scheme (BATS) version 1e as coupled to NCAR Community Climate Model. NCAR Tech. Note, 387+STR, 72 pp. [Available from UCAR Communications, P.O. Box 3000, Boulder, CO 80307-3000.]

Giorgi, F., M. R. Marinucci, G. T. Bates, and G. De Canio, 1993a: Development of a second-generation regional climate model (RegCM2). Part I: Boundary-layer and radiative transfer. *Mon. Wea. Rev.,* **121,** 2794–2813.

——, ——, ——, and ——, 1993b: Development of a second-generation regional climate model (RegCM2). Part II: Convective processes and assimilation of boundary conditions. *Mon. Wea. Rev.,* **121,** 2814–2832.

——, L. Mearns, C. Shields, and L. Mayer, 1996: A regional model study of the importance of local versus remote controls of the 1988 drought and the 1993 flood over the central United States. *J. Climate,* **9,** 1150–1162.

Grell, G. A., 1993: Prognostic evaluation of assumptions used by cumulus parameterizations. *Mon. Wea. Rev.,* **121,** 764–787.

Horel, J. D., J. B. Pechamann, A. N. Hahmann, and J. E. Geisler, 1994: Simulation of the Amazon Basin circulation with a regional model. *J. Climate,* **7,** 56–71.

Jones, R. G., J. M. Murphy, and M. Noguer, 1995: Simulation of climate change over Europe using a nested regional-climate model. Part I: Assessment of control climate, including sensitivity to location of boundaries. *Quart. J. Roy. Meteor. Soc.,* **121,** 1413–1450.

Kida, H., T. Koide, H. Sasaki, and M. Chiba, 1991: A new approach for coupling a limited area model to a GCM for regional climate simulations. *J. Meteor. Soc. Japan,* **69,** 723–728.

Kuo, S. L., 1974: Further studies of the parameterization of the effect of cumulus convection on large-scale flow. *J. Atmos. Sci.,* **31,** 1232–1240.

Mo, K. C., J. N. Paegle, and J. Paegle, 1995: Physical mechanisms of the 1993 floods. *J. Atmos. Sci.,* **52,** 879–895.

Paegle, J., K. C. Mo, and J. N. Paegle, 1996: Dependence of simulated precipitation on surface evaporation during the 1993 United States summer floods. *Mon. Wea. Rev.,* **124,** 345–361.

Pan, Z., M. Segal, R. Turner, and E. Takle, 1995: Model simulation of impacts of transient surface wetness on summer rainfall in the United States Midwest during drought and flood years. *Mon. Wea. Rev.,* **123,** 1575–1581.

——, E. Takle, M. Segal, and R. Turner, 1996: Influences of model parameterization schemes on the response of rainfall to soil moisture in the central United States. *Mon. Wea. Rev.,* **124,** 1786–1802.

Renshaw, E., and E. D. Ford, 1983: The interpretation of process from pattern using two-dimensional spectral analysis: Methods and problems of interpretation. *Appl. Stat.,* **32,** 51–63.

Rodenhuis, D. R., D. Miskus, G. D. Bell, and K. C. Mo, 1994: Meteorological flood origin, description, and causes of the Great Flood of 1993. Preprints, *Symp. on the Great Flood of 1993,* Nashville, TN, Amer. Meteor. Soc., 1–12 pp.

Yap, K.-S., 1995: Impact of a Newtonian assimilation and physical initialization on the initialization and prediction by a tropical mesoscale model. *Mon. Wea. Rev.,* **123,** 833–861.